JACS
JOURNAL OF THE AMERICAN CHEMICAL SOCIETY
Article
pubs.acs.org/JACS

Pillar[6]arene-Based Photoresponsive Host–Guest Complexation

Guocan Yu,[†] Chengyou Han,[†] Zibin Zhang,[†] Jianzhuang Chen,[†] Xuzhou Yan,[†] Bo Zheng,[†] Shiyong Liu,*[,‡] and Feihe Huang*[,†]

[†]Department of Chemistry, Zhejiang University, Hangzhou 310027, People's Republic of China

[‡]Hefei National Laboratory of Physical Sciences at the Microscale, CAS Key Laboratory of Soft Matter Chemistry, Department of Polymer Science and Engineering, University of Science and Technology of China, Hefei, Anhui 230026, People's Republic of China

Supporting Information

ABSTRACT: The *trans* form of an azobenzene-containing guest can complex with a pillar[6]arene, while it cannot complex with pillar[5]arenes due to the different cavity sizes of the pillar[6]arene and the pillar[5]arenes. The spontaneous aggregation of its host–guest complex with the pillar[6]arene can be reversibly photocontrolled by irradiation with UV and visible light, leading to a switch between irregular aggregates and vesicle-like aggregates. This new pillar[6]arene-based photoresponsive host–guest recognition motif can work in organic solvents and is a good supplement to the existing widely used cyclodextrin/azobenzene recognition motif.

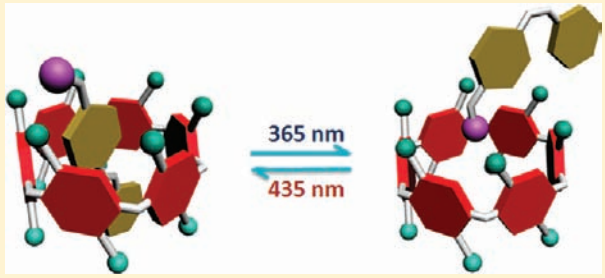

1. INTRODUCTION

Stimuli-responsive host–guest systems have attracted much interest due to their application in a broad range of fields, such as memory storage, smart supramolecular polymers, drug delivery systems, sensors, protein probes, and functional nanodevices.[1] Numerous external stimuli such as temperature-change, pH-change, redox, and light have been utilized in these systems.[2] Among them, light is of special interest because it can work rapidly, remotely, cleanly, and noninvasively.[3] A variety of photoresponsive groups have been utilized as switching units to control the microscopic structures and relevant functions of various supramolecular systems.[4] Among them, azobenzene has been proved to be especially advantageous for inducing dramatic structural changes in supramolecular systems due to its photoinduced *E*/*Z* isomerization, accompanied by large molecular property changes.[5]

Pillararenes are a new type of macrocyclic hosts. Their repeating units are connected by methylene bridges at the *para*-positions, forming a unique rigid pillar architecture, which is different from the basket-shaped structure of *meta*-bridged calixarenes. The unique structure and easy functionalization of pillararenes have afforded them outstanding ability to selectively bind different kinds of guests and provided a useful platform for the construction of various interesting supramolecular systems, including cyclic dimers, chemosensors, supramolecular polymers, and transmembrane channels.[6,7] They have been described as "fascinating cyclophanes with a bright future".[6p] Until now, two kinds of pillararenes, pillar[5]arenes and pillar[6]arenes, containing five and six units, respectively, have been reported.[6−8] The host–guest chemistry of pillar[5]arenes has been widely explored. However, the host–guest chemistry of pillar[6]arenes has been rarely investigated.[7b,d,8] Furthermore, pillar[6]arene-based photoresponsive host–guest complexation has not been reported yet. Herein, we investigate the complexation of an azobenzene-containing guest **3** with pillar[5]arenes **1a**, **1b**, and **1c** and pillar[6]arene **2**. Because of the different cavity sizes of the pillar[5]arenes and the pillar[6]arene, *trans*-**3** cannot complex with the pillar[5]arenes **1**, while it can reside in the cavity of the pillar[6]arene **2**. A photoresponsive threading–dethreading switch can be achieved upon UV and visible light irradiation due to the *trans*–*cis* photoisomerization of **3**, accompanied by disassembly and assembly of the corresponding aggregates.

2. EXPERIMENTAL SECTION

Synthetic Procedures (See Scheme S1 in the Supporting Information). Pillar[5]arenes **1a**, **1b**, and **1c** and pillar[6]arene **2** were reported previously.[6b,8]

For the synthesis of **3**, a solution of 4-bromomethylazobenzene **B** (5.40 g, 19.7 mmol) in ethanol (50.0 mL) and trimethylamine (30% in ethanol, 50.0 mL) was allowed to react at 80 °C for 24 h. The solution was concentrated under reduced pressure. The residue was diluted with water (20.0 mL) and washed with dichloromethane (5 × 5 mL). Excess NH_4PF_6 was added to the aqueous solution to produce an orange precipitate, which was collected by filtration and washed with water to give **3** as an orange solid (6.54 g, 86%). mp 216.5–217.8 °C. The proton NMR spectrum of **3** is shown in Figure S1. ^{1}H NMR (500 MHz, 10:1 chloroform-*d*/acetonitrile-d_3, room temperature) δ (ppm): 7.99 (d, J = 8.0 Hz, 2H), 7.93 (d, J = 8.0 Hz, 2H), 7.63 (d, J = 8.0 Hz, 2H), 7.52 (s, 3H), 4.54 (s, 2H), 3.16 (s, 9H). The ^{13}C NMR spectrum of **3** is shown in Figure S2. ^{13}C NMR (125 MHz, acetonitrile-d_3, room temperature) δ (ppm): 153.38, 152.16, 133.76, 131.67, 129.86, 129.17,

Received: March 28, 2012
Published: April 27, 2012

   dx.doi.org/10.1021/ja302998q | *J. Am. Chem. Soc.* 2012, 134, 8711–8717

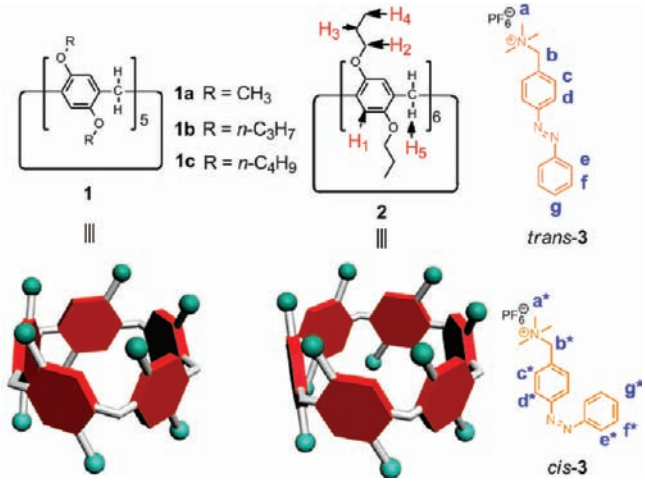

122.74, 122.55, 117.04, 68.44, 54.93, 54.90, 54.86, 52.26, 52.23, 52.19, 51.36. LRESIMS is shown in Figure S3: m/z 253.9 $[M - PF_6]^+$ (100%). HRESIMS: m/z calcd for $[M - PF_6]^+$ $C_{16}H_{20}N_3$, 254.1652; found 254.1641; error −4.3 ppm.

Preparation of Scanning Electron Microscopy (SEM) Samples. The SEM samples were prepared on clean Si substrates. Each sample solution was deposited onto a Si substrate, placed in a refrigerator for 30 min, and freeze-dried in a freeze-drying machine at −20 °C under reduced pressure.

Transmission Electron Microscopy (TEM) and Dynamic Light Scattering (DLS) Studies. The self-assembled structures of *trans*-**3**, **2**⊃*trans*-**3**, and **2**⊃*cis*-**3** were revealed using TEM. An equimolar solution of 5.00×10^{-4} M **2** and *trans*-**3** was made first in a mixture of $CHCl_3$ and CH_3CN (v:v, 10:1). The samples of **2**⊃*trans*-**3** were prepared by drop-coating this solution onto a carbon-coated copper grid, while the samples of **2**⊃*cis*-**3** were prepared by drop-coating this solution on a carbon-coated copper grid under the irradiation of UV light until the solvent evaporated. TEM experiments were performed on a JEM-1200EX instrument. The solution of *trans*-**3** (5.00×10^{-4} M) was left to stand overnight before being used for DLS tests, while for a solution of **2** (5.00×10^{-4} M) and *trans*-**3** (5.00×10^{-4} M), it was left to stand overnight and irradiated by UV light for 10 min before being used for DLS tests. The irregular aggregates in solution were eliminated by using a microporous membrane. The diameters of the assemblies were measured on a Nano-ZS ZEN3600 instrument.

Critical Aggregation Concentration (CAC) Determination of *trans*-3. Some parameters such as the conductivity, osmotic pressure, fluorescence intensity, and surface tension of the solution change sharply around the critical aggregation concentration. The dependence of the solution conductivity on the solution concentration is used to determine the critical aggregation concentration. Typically, the slope of the change in conductivity versus the concentration below CAC is steeper than the slope above the CAC. Therefore, the junction of the conductivity−concentration plot represents the CAC value. To measure the CAC of *trans*-**3**, the conductivities of the solutions at different concentrations (from 0 to 0.63 mM) were determined, and by plotting the changes of the conductivity versus the concentration, we could get the critical aggregation concentration (CAC) of *trans*-**3**.

Crystallography. *X-ray Crystal Data of* ***P5***. Crystallographic data: colorless, $C_{65}H_{90}O_{10}$, FW 1031.37, triclinic, space group $P\bar{1}$, a = 12.1787(4), b = 13.9544(5), c = 20.7259(7) Å, α = 80.666(3)°, β = 83.051(3)°, γ = 81.950(3)°, V = 3424.0(2) Å^3, Z = 2, D_c = 1.000 g cm^{-3}, T = 100 K, μ = 0.522 mm^{-1}, 46 719 measured reflections, 12081 independent reflections, 691 parameters, 0 restraints, $F(000)$ = 1120, R_1 = 0.0932, wR_2 = 0.2714 (all data), R_1 = 0.0815, wR_2 = 0.2547 [$I > 2\sigma(I)$], max. residual density 0.759 e·Å^{-3}, and goodness-of-fit (F^2) = 1.054. CCDC-851275.

X-ray Crystal Data of ***P6***. Crystallographic data: colorless, $C_{78}H_{108}O_{12}$, FW 1237.64, triclinic, space group $P\bar{1}$, a = 13.2244(10), b = 13.7845(10), c = 23.3051(12) Å, α = 89.203(5)°, β = 79.553(5)°, γ = 76.373(6)°, V = 4058.4(5) Å^3, Z = 2, D_c = 1.013 g cm^{-3}, T = 293 K, μ = 0.529 mm^{-1}, 27 170 measured reflections, 13 739 independent reflections, 823 parameters, 11 restraints, $F(000)$ = 1344, R_1 = 0.1758, wR_2 = 0.4244 (all data), R_1 = 0.1400, wR_2 = 0.3813 [$I > 2\sigma(I)$], max. residual density 0.818 e·Å^{-3}, and goodness-of-fit (F^2) = 1.450. CCDC-851276.

3. RESULTS AND DISCUSSION

Host−Guest Studies. The complexation of *trans*-**3** with pillar[5]arenes **1a**, **1b**, and **1c** and pillar[6]arene **2** was studied by ^{1}H NMR spectroscopy first. As shown in Figure 1, when 1.0 equiv of **1a**, **1b**, or **1c** was added to a solution of *trans*-**3**, no chemical shift changes were observed for protons of *trans*-**3**. However, upon addition of 1.0 equiv of pillar[6]arene **2**, chemical shift changes of some protons on *trans*-**3** appeared. Protons H_d shifted upfield from 7.98 to 7.71 ppm ($\Delta\delta$ = −0.27 ppm). The resonance peaks related to H_a, H_b, and H_c disappeared after complexation (spectrum e in Figure 1). The reason is that these protons are located within the cavity of **2** and shielded by the electron-rich cyclic structure upon forming a threaded structure between **2** and *trans*-**3**. Extensive broadening effect occurred due to complexation dynamics.[6d] In addition, no chemical shift changes happened for protons H_e and slight chemical shift changes occurred for protons H_f and H_g, indicating that they are not involved in the noncovalent interactions between **2** and *trans*-**3** because *trans*-**3** is too long to be wrapped by host **2** completely. On the other hand, the protons on pillar[6]arene **2** also exhibited slight chemical shift changes due to the interactions between *trans*-**3** and **2**. The peak related to H_1 on the benzene rings shifted downfield slightly. The signals corresponding to H_2 and H_5 shifted upfield −0.07 and −0.04 ppm, respectively. 2D NOESY NMR spectrum is a useful tool to study the relative positions of the components in host−guest inclusion complexes, so it was further used to investigate the complexation between **2** and *trans*-**3**. NOE correlation signals were observed between protons H_d on the azobenzene unit of *trans*-**3** and protons H_1 on pillar[6]arene **2** as well as the bridging methylene protons H_5 (**A** and **B** in Figure S11). On the other hand, no

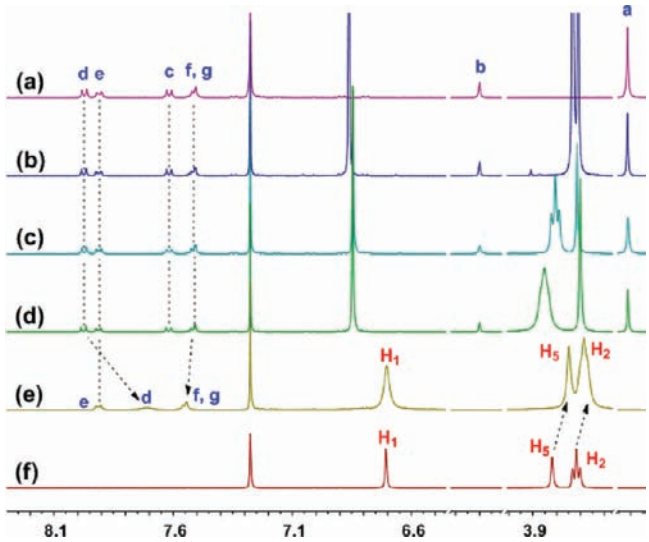

Figure 1. Partial ^{1}H NMR spectra (500 MHz, 10:1 chloroform-*d*/acetonitrile-d_3, room temperature) of 2.00 mM *trans*-**3** (a), 2.00 mM *trans*-**3** and **1a** (b), 2.00 mM *trans*-**3** and **1b** (c), 2.00 mM *trans*-**3** and **1c** (d), 2.00 mM *trans*-**3** and **2** (e), and 2.00 mM **2** (f).

NOE correlation signals were observed between protons H_{e-g} on the guest and the protons on the pillar[6]arene **2**.

Single crystals of pillar[5]arene **1b** and pillar[6]arene **2** were obtained by slow evaporation of their respective solutions in a mixture of dichloromethane and acetonitrile (1:2, v/v). Although pillar[5]arene **1b** and pillar[6]arene **2** have the same repeating unit and are cyclic molecules, their X-ray crystal structures (Figure 2) have an obvious difference. Pillar[5]arenes

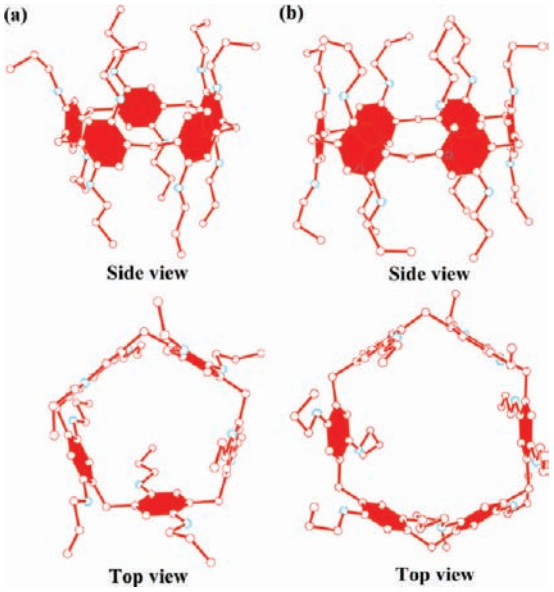

Figure 2. Ball-stick views of the crystal structures of **1b** (a) and **2** (b). Hydrogens and the solvent molecules were omitted for clarity. Carbon atoms are red, and oxygen atoms are blue.

1b has a pentagon-like cyclic structure, while pillar[6]arene **2** has a hexagon-like cyclic structure. By treating pillar[5]arenes and pillar[6]arene as a regular pentagonal pillar and a regular hexagonal pillar, respectively, and ignoring the influence of the substituents on the oxygen atoms of the benzene rings, we calculated the structural parameters of pillar[5]arenes and pillar[6]arene (Figure S18). In terms of the cavity size, the diameter of the internal cavity of pillar[5]arenes is ~4.7 Å, equal to that of α-cyclodextrin (~4.7 Å).[9] The diameter of the internal cavity of pillar[6]arene is ~6.7 Å, close to that of β-cyclodextrin (~6.0 Å).[9] These phenomena mentioned above suggested that due to the difference in cavity sizes between pillar[5]arenes **1** and pillar[6]arene **2** (Figures 2 and S18), the azobenzene-containing guest *trans*-**3** could not complex with pillar[5]arenes **1**, while it could thread into the cavity of pillar[6]arene **2** to form a [2]pseudorotaxane **2**⊃*trans*-**3** (its cartoon representation is shown in Figure 4) with its positive trimethylammonium group close to the oxygen atoms on pillar[6]arene **2**, the benzene ring containing H_c and H_d located in the cavity of pillar[6]arene **2**, and the other benzene ring outside of the cavity. The interactions between pillar[6]arene **2** and *trans*-**3** might include hydrogen bonds and $\pi-\pi$ stacking interactions. It should be noted that, although pillar[5]arenes **1** and α-cyclodextrin have similar internal cavity size, pillar[5]arenes **1** cannot complex *trans*-**3**, while α-cyclodextrin can bind azobenzene derivatives in water.[9] A possible reason is that pillar[5]arenes **1** have a rigid pillar structure, while α-cyclodextrin has a flexible truncated conic structure.

A mole ratio plot (Figure S13) based on the proton NMR data of H_d on **2** demonstrated that the complex between **2** and *trans*-**3** has 1:1 stoichiometry in 10:1 (v/v) chloroform/acetonitrile. The ESI-MS experiments confirmed the formation of a 1:1 complex between **2** and *trans*-**3**. The relevant peak was found at m/z 1493.1 (Figure S9), corresponding to $[\mathbf{2}\supset trans\text{-}\mathbf{3}-PF_6]^+$. Peaks related to other stoichiometries were not found. ^{1}H NMR titration experiments were carried out in 10:1 chloroform-d/acetonitrile-d_3 to investigate the binding abilities between **2** and *tran*-**3** (Figure S12). The association constant (K_a) of **2**⊃*trans*-**3** was determined to be $(2.22 \pm 0.34) \times 10^3$ M^{-1} by fitting the chemical shift changes of H_d on the guest as a function of the initial concentration of **2** (Figure S14).

As expected, the azobenzene-containing guest **3** exhibited good photoresponsive properties as investigated by UV−vis spectroscopy (Figures 3 and S4). Upon irradiation with UV light at 365 nm, the absorption band at around 318 nm decreased remarkably, and concomitantly the band at around 435 nm increased slightly. The absorption bands of the azobenzene unit at 318 and 435 nm are ascribed to $\pi-\pi^*$ and

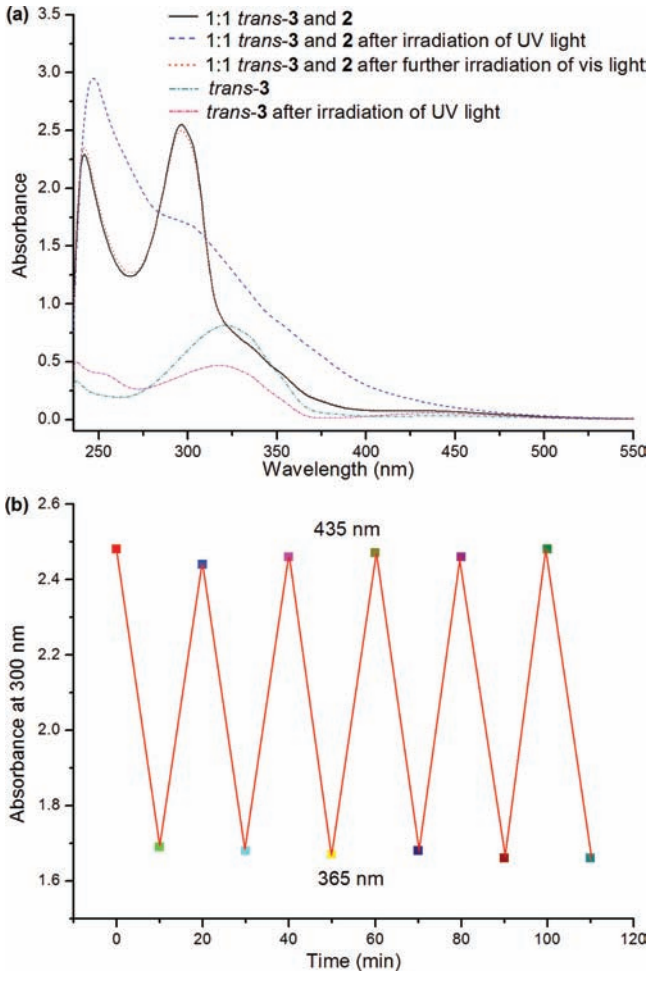

Figure 3. (a) UV−vis spectra (10:1 chloroform/acetonitrile, v/v) of 5.00×10^{-4} M *trans*-**3** (initial and after irradiation with UV light at 365 nm for 3 min) and an equimolar solution of 5.00×10^{-4} M *trans*-**3** and **2** (initial, after irradiation with UV light at 365 nm for 3 min, and then after irradiation with visible light at 435 nm for 10 min) and (b) changes of the absorbance at 300 nm of an equimolar solution of **2** and *trans*-**3** upon alternating irradiation with UV and visible light for 10 min.

dx.doi.org/10.1021/ja302998q | J. Am. Chem. Soc. 2012, 134, 8711−8717

n−π^* transitions, respectively. The changes of the absorption bands induced by UV irradiation indicated the photoisomerization from the *trans*-**3** state to the *cis*-**3** state. On the contrary, upon irradiation with visible light at 435 nm, the absorption peak at 435 nm attributable to *cis*-**3** decreased, while the absorption band at 318 nm corresponding to *trans*-**3** increased, indicating a change from the *cis*-**3** form to the *trans*-**3** form.

Usually, the photoisomerization of the azobenzene group proceeds with first-order kinetics in solution,[4e,5b] so the interaction between pillar[6]arene **2** and *trans*-**3** can be further validated by the photoisomerization process. By plotting the changes of absorbance versus time, the initial *trans*−*cis* photoisomerization rate constant (k_t) of **3** could be obtained as 0.090 ± 0.009 s^{-1}, while the value of k_t decreased considerably to 0.067 ± 0.006, 0.061 ± 0.004, and 0.020 ± 0.002 s^{-1}, respectively (Figure S8), in the presence of 0.5, 0.8, and 1.0 equiv of pillar[6]arene **2**. Accompanied by the increase of **2**, the *trans*−*cis* photoisomerization rate constants (k_t) of **3** decreased. The K_a value of **2**⊃*cis*-**3** was determined to be (2.64 ± 0.29) × 10^2 M^{-1} by employing ^{1}H NMR titration experiments (Figure S17), which was lower than that of **2**⊃*trans*-**3**. The reason that the photoisomerization rate constant decreased upon addition of **2** could be as follows: in the absence of **2**, *trans*-**3** molecules freely disperse in solution so they can undergo the *trans*−*cis* conversion easily. When host **2** is added into the solution of *trans*-**3**, an inclusion complex of pillar[6]arene **2** and *trans*-**3** forms in which the macrocyclic host encircled the axle. Subsequently, UV light irradiation can convert the conformation of uncomplexed *trans*-**3** molecules from the *trans* form to the *cis* form, but the photoisomerization of complexed *trans*-**3** molecules is geometrically restricted. It is this restructuring of the energy landscape for the system that resulted in the reduction of the photoisomerization rate constant.[5b]

Comparing the sizes of **3** and pillar[6]arene **2** (Figure S18), we know that *cis*-**3** is larger than the cavity of pillar[6]arene **2**. Therefore, upon irradiation with UV light, the conformation of some *trans*-**3** molecules changed from the *trans* state to the *cis* state, and these **3** molecules could not thread into the cavity of **2** anymore. As shown in Figure 3a, the absorption band at 300 nm of an equimolar solution of **2** and *trans*-**3** decreased obviously after irradiation by UV light at 365 nm for 3 min. The decreased absorption was caused by the *trans*−*cis* isomerization of *trans*-**3** molecules. The absorption intensity at 300 nm could be recovered to the initial state after irradiation by visible light at 435 nm for 10 min. Upon alternately exposing an equimolar solution of **2** and *trans*-**3** to light at 365 and 435 nm, this reversible photoisomerization process could be recycled many times (Figure 3b). It indicated that this threading/dethreading transition could be controlled reversibly by irradiation with UV and visible light due to the *trans*−*cis* photoisomerization of **3**. UV spectroscopic titrations were also performed to verify the interactions between *trans*-**3** and **2** in solution. Upon addition of **2** to a solution of 5.00 × 10^{-4} M *trans*-**3**, a blue shift of the maximum absorption peak from 318 to 294 nm was observed (Figure S25a). On the contrary, a red shift occurred upon addition of *trans*-**3** to a solution of 5.00 × 10^{-4} M **2** (Figure S25b). These shifts confirmed the host−guest complexation between **2** and *trans*-**3**.

Photocontrolled Threading−Dethreading Switch. To further confirm this hypothesis, ^{1}H NMR characterization was conducted to provide evidence about the interaction of *trans*-**3** and *cis*-**3** with pillar[6]arene **2**. Normally, azobenzene derivatives prefer the *trans* form in solution (spectrum b in Figure 4). When a solution of *trans*-**3** was irradiated by UV light

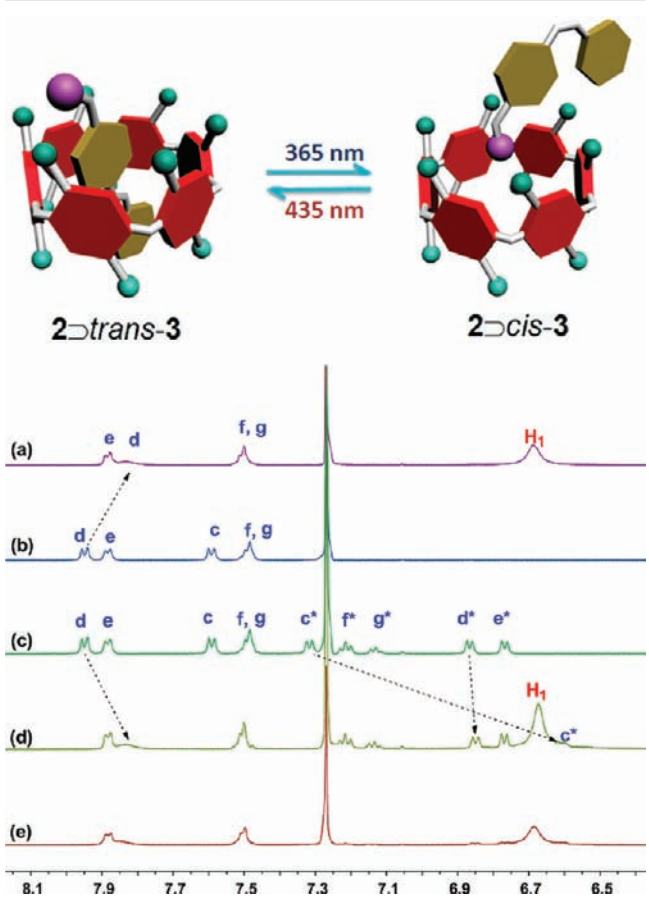

Figure 4. Partial ^{1}H NMR spectra (500 MHz, 10:1 chloroform-*d*/acetonitrile-d_3, room temperature) of 2.00 mM *trans*-**3** and **2** (a), 2.00 mM *trans*-**3** (b), 2.00 mM *trans*-**3** after irradiation at 365 nm for 10 min (c), 2.00 mM *trans*-**3** and **2** after irradiation at 365 nm for 10 min (d), and then after further irradiation at 450 nm for 10 min (e).

for 10 min, the ratio of the *trans* to *cis* form changed to about 50:50 (spectrum c in Figure 4). When the solution comprised of equimolar amounts of *trans*-**3** and **2** was irradiated by UV light for 10 min, the chemical shifts of the protons H_{c*} on the π-electron rich benzene ring of *cis*-**3** shifted upfield dramatically from 7.33 to 6.61 ppm, and the peak related to protons H_{d*} shifted upfield from 6.87 to 6.85 ppm (spectra c and d in Figure 4). On the other hand, the peaks related to H_{a*} and H_{b*} shifted upfield slightly ($\Delta\delta$ = −0.11 and −0.10 ppm, respectively) and exhibited broadening effect (Figure S20). On the contrary, the chemical shifts of protons H_{e*}, H_{f*}, and H_{g*} on the benzene rings did not change (spectra c and d in Figure 4). These phenomena indicated that the trimethylammonium group on the *cis*-**3** was bound by a rim of pillar[6]arene **2**, while the rest of guest *cis*-**3** was outside the cavity of **2** as shown by a cartoon representation of **2**⊃*cis*-**3** in Figure 4. Upon irradiation with light at 450 nm for sufficient time, *cis*-**3** was converted back to *trans*-**3**, and the proton signals of spectrum e in Figure 4 were the same as those of spectrum a in Figure 4.

Microstructures of the Self-Assembled Aggregates. We further explored how the presence of pillar[6]arene **2** and photoirradiation affects the aggregation of **3**. The critical aggregation concentration of the *trans*-**3** was measured to be

dx.doi.org/10.1021/ja302998q | J. Am. Chem. Soc. 2012, 134, 8711−8717

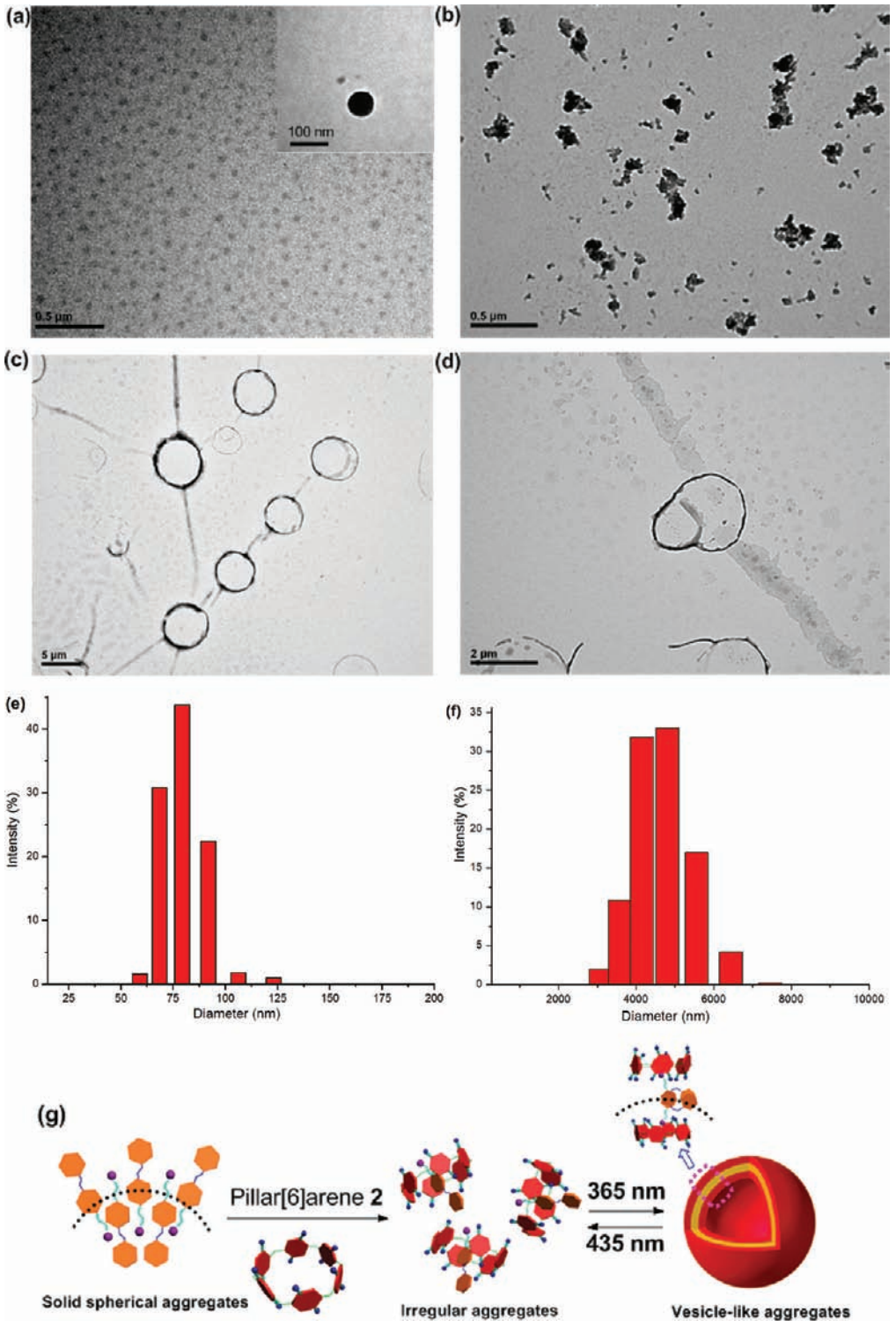

Figure 5. TEM images of *trans*-**3** (a, the scale bar is 0.5 μm) with an inset showing an enlarged image (the scale bar is 100 nm), an equimolar mixture of *trans*-**3** and pillar[6]arene **2** (b, the scale bar is 0.5 μm), and an equimolar mixture of *trans*-**3** and pillar[6]arene **2** after irradiation at 365 nm for 10 min (c, the scale bar is 5 μm), the fusion process from small-size vesicle-like aggregates to large-size vesicle-like aggregates (d, the scale bar is 2 μm), DLS results of *trans*-**3** solution (e) and the aggregates of **2**⊃*cis*-**3** (f), and the illustration of the formation of the aggregates (g). The concentration of *trans*-**3** was 5.00×10^{-4} M, which is larger than the critical aggregation concentration, 1.68×10^{-4} M of *trans*-**3**.

1.68×10^{-4} M (Figure S21). For some amphiphiles, such as cetyltrimethylammonium bromide, it has been reported that their aggregration can be reversibly controlled due to the controlled formation of inclusion complexes with cyclodextrins in water.[10] As shown by a TEM image in Figure 4a, *trans*-**3** formed solid spherical aggregates with an average diameter about 90 nm, which was further verified by SEM experiments (Figure S22a). When an equimolar amount of pillar[6]arene **2** was added, *trans*-**3** threaded into the cavity of **2** to form inclusion complex **2**⊃*trans*-**3**, resulting in the disappearance of

dx.doi.org/10.1021/ja302998q | *J. Am. Chem. Soc.* 2012, 134, 8711−8717

the solid spherical aggregates of *trans*-**3** (Figure 4b). Interestingly, when the above system was irradiated by UV light at 365 nm, vesicle-like aggregates with a diameter of about 5 μm (Figure 4c) appeared. These vesicle-like aggregates presumably came from the self-assembly of unthreaded host–guest complex **2**⊃*cis*-**3**. It should be noted that irregular aggregates from the inclusion complex **2**⊃*trans*-**3** can be still observed as black dots in Figure 4c because not all of the *trans*-**3** molecules were converted to the *cis*-**3** molecules by the UV irradiation. On the other hand, the fusion process from small-size vesicle-like aggregates to large-size vesicle-like aggregates was also found in TEM images (Figure 4d). As shown by DLS, the main diameter distribution of the solid spherical aggregates formed from *trans*-**3** is around 78 nm (Figure 5e), while the main diameter distribution for the vesicle-like aggregates formed from the unthreaded inclusion complexes between *cis*-**3** and **2** is about 4.8 μm (Figure 5f). The results determined by DLS were in good agreement with the TEM images in Figure 4a and c. Small-angle X-ray scattering (SAXS) was used to clarify the packing of the *cis*-**3** and pillar[6]arene **2** complex in the vesicle-like aggregates (Figure S24). The thickness of the bilayer of the vesicle-like aggregates was calculated to be 1.7 nm by SAXS and around 2.0 nm from the TEM experiments (Figure S22b), in accordance with the length of two **2**⊃*cis*-**3** inclusion complexes with antiparallel packing. Moreover, the vesicle-like aggregates disassembled upon irradiation with visible light at 450 nm, and reformed on subsequent UV irradiation at 365 nm. These irregular aggregates and vesicle-like aggregates can be obtained by UV and visible light irradiation reversibly, which results from the threading and dethreading of the cavity of pillar[6]arene **2** by the photoresponsive guest **3**. A possible mechanism for this aggregation control is shown in Figure 4g. In the mixture of chloroform and acetonitrile (10/1, v/v), the azobenzene part of *trans*-**3** is solvophilic, while the trimethyl ammonium moiety of *trans*-**3** is solvophobic. Furthermore, hydrogen bonding between the hydrogen atoms on the trimethyl ammonium group and the nitrogen atoms can provide an additional driving force for the aggregation of *trans*-**3** (Figure S23). Therefore, it can self-assemble to form solid spherical aggregates shown in Figure 4a. When solvophilic pillar[6]arene **2** is added, a threaded inclusion complex **2**⊃*trans*-**3** forms with the solvophobic trimethyl ammonium moiety included in the cavity of **2** so the regular aggregates of amphiphilic *trans*-**3** in Figure 4a are destroyed to form irregular aggregates in Figure 4b. When this solution is irradiated with UV light, some *trans*-**3** molecules are converted into *cis*-**3**, so two host–guest complexes, threaded **2**⊃*trans*-**3** and unthreaded **2**⊃*cis*-**3**, exist in solution. Threaded **2**⊃*trans*-**3** is solvophilic. However, the two ends of unthreaded **2**⊃*cis*-**3** are solvophilic, while its middle part is solvophobic because the solvophobic trimethyl ammonium moiety is not included in the cavity of pillar[6]arene **2**. Therefore, both vesicle-like aggregates from self-assembly of unthreaded **2**⊃*cis*-**3** and irregular aggregates from self-assembly of threaded **2**⊃*trans*-**3** can be observed in Figure 4c. It should be noted that the fusion process shown in Figure 4d is a typical intermediate state, supporting that this mechanism is plausible.[3h,5d]

4. CONCLUSIONS

The cavity size of pillar[6]arene **2** is suitable for the azobenzene-containing guest *trans*-**3**, while the cavity size of pillar[5]arenes **1** is too small for *trans*-**3**. Upon irradiation with UV light, the conformation of **3** changes from the *trans* form to the *cis* form, and the threading of **3** through the cavity of pillar[6]arene **2** is prohibited due to the size mismatch, but it can rethread through the cavity again upon visible light irradiation. This photocontrolled switch of threading results in microstructural changes of the self-assembled aggregates formed from the host–guest inclusion complex between **2** and **3**. These phenomena have been demonstrated by various characterization techniques. Therefore, this new efficient pillar[6]arene-based host–guest recognition motif exhibited a photoresponsive threading–dethreading switch in organic solvents. Acting as a good supplement to the existing widely used cyclodextrin/azobenzene recognition motif in water, it will have a broad application in the future fabrication of more sophisticated photoresponsive supramolecular systems.

■ ASSOCIATED CONTENT

Supporting Information

Experimental details, NMR spectra, SEM images, and X-ray crystallographic files (CIF) for **1b** and **2** and other materials. This material is available free of charge via the Internet at http://pubs.acs.org.

■ AUTHOR INFORMATION

Corresponding Author

sliu@ustc.edu.cn; fhuang@zju.edu.cn

Notes

The authors declare no competing financial interest.

■ ACKNOWLEDGMENTS

The National Natural Science Foundation of China (20834004, 91027006, 21125417), the Fundamental Research Funds for the Central Universities (2012QNA3013), and the Zhejiang Provincial Natural Science Foundation of China (R4100009) are greatly acknowledged for their generous financial support.

■ REFERENCES

(1) (a) Livoreil, A.; Dietrich-Buchecker, C. O.; Sauvage, J.-P. *J. Am. Chem. Soc.* **1994**, *116*, 9399–9400. (b) Kelly, T. R.; Silva, H. D.; Silva, R. A. *Nature* **1999**, *401*, 150–152. (c) Koumura, N.; Zijlstra, R. W. J.; van Delden, R. A.; Harada, N.; Feringa, B. L. *Nature* **1999**, *401*, 152–155. (d) Jeon, Y. J.; Bharadwaj, P. K.; Choi, S. W.; Lee, J. W.; Kim, K. *Angew. Chem., Int. Ed.* **2002**, *41*, 4474–4476. (e) Muraoka, T.; Kinbara, K.; Kobayashi, Y.; Aida, T. *J. Am. Chem. Soc.* **2003**, *125*, 5612–5613. (f) Kay, E. R.; Leigh, D. A.; Zerbetto, F. *Angew. Chem., Int. Ed.* **2007**, *46*, 72–191. (g) Niu, Z.; Gibson, H. W. *Chem. Rev.* **2009**, *109*, 6024–6046. (h) Ge, Z.; Hu, J.; Huang, F.; Liu, S. *Angew. Chem., Int. Ed.* **2009**, *48*, 1798–1902. (i) Wang, F.; Zhang, J.; Ding, X.; Dong, S.; Liu, M.; Zheng, B.; Li, S.; Wu, L.; Yu, Y.; Gibson, H. W.; Huang, F. *Angew. Chem., Int. Ed.* **2010**, *49*, 1090–1094. (j) Cao, D.; Amelia, M.; Klivansky, L. M.; Koshkakaryan, G.; Khan, S. I.; Semeraro, M.; Silvi, S.; Venturi, M.; Credi, A.; Liu, Y. *J. Am. Chem. Soc.* **2010**, *132*, 1110–1122. (k) Li, Y.; Park, T.; Quansah, J. K.; Zimmerman, S. C. *J. Am. Chem. Soc.* **2011**, *133*, 17118–17121. (l) Niu, Z.; Huang, F.; Gibson, H. W. *J. Am. Chem. Soc.* **2011**, *133*, 2836–2839.

(2) (a) Sauvage, J.-P. *Acc. Chem. Res.* **1998**, *31*, 611–619. (b) Armaroli, N.; Balzani, V.; Collin, J.-P.; Gaviña, P.; Sauvage, J.-P.; Ventura, B. *J. Am. Chem. Soc.* **1999**, *121*, 4397–4480. (c) Philip, I. E.; Kaifer, A. E. *J. Am. Chem. Soc.* **2002**, *124*, 12678–12679. (d) Jones, J. W.; Bryant, W. S.; Bosman, A. W.; Janssen, R. A. J.; Meijer, E. W.; Gibson, H. W. *J. Org. Chem.* **2003**, *68*, 2385–2389. (e) Tian, H.; Qin, B.; Yao, R.; Zhao, X.; Yang, S. *Adv. Mater.* **2003**, *15*, 2104–2107. (f) Moon, K.; Kaifer, A. E. *J. Am. Chem. Soc.* **2004**, *126*, 15016–15017. (g) Moon, K.; Grindstaff, J.; Sobransingh, D.; Kaifer, A. E. *Angew. Chem., Int. Ed.* **2004**, *43*, 5496–5499. (h) Vella, S. J.; Tiburcio, J.;

Gauld, J. W.; Loeb, S. J. *Org. Lett.* **2006**, *8*, 3421−3424. (i) Dong, S.; Luo, Y.; Yan, X.; Zheng, B.; Ding, X.; Yu, Y.; Ma, Z.; Zhao, Q.; Huang, F. *Angew. Chem., Int. Ed.* **2011**, *51*, 1905−1909. (j) Du, P.; Liu, J.; Chen, G.; Jiang, M. *Langmuir* **2011**, *27*, 9602−9608.

(3) (a) Altieri, A.; Gatti, F. G.; Kay, E. R.; Leigh, D. A.; Martel, D.; Paolucci, F.; Slawin, A. M. Z.; Wong, J. K. Y. *J. Am. Chem. Soc.* **2003**, *125*, 8644−8654. (b) Altieri, A.; Bottari, G.; Dehez, F.; Leigh, D. A.; Wong, J. K. Y.; Zerbetto, F. *Angew. Chem., Int. Ed.* **2003**, *42*, 2296−2300. (c) Bottari, G.; Dehez, F.; Leigh, D. A.; Nash, P. J.; Pérez, E. M.; Wong, J. K. Y.; Zerbetto, F. *Angew. Chem., Int. Ed.* **2003**, *42*, 5886−5889. (d) Pérez, E. M.; Dryden, D. T. F.; Leigh, D. A.; Teobaldi, G.; Zerbetto, F. *J. Am. Chem. Soc.* **2004**, *126*, 12210−12211. (e) Qu, D. H.; Wang, Q.-C.; Ren, J.; Tian, H. *Org. Lett.* **2004**, *6*, 2085−2088. (f) Davidson, G. J. E.; Loeb, S. J.; Passaniti, P.; Silvi, S.; Credi, A. *Chem.-Eur. J.* **2006**, *12*, 3233−3242. (g) Vella, S. J.; Tiburcio, J.; Loeb, S. J. *Chem. Commun.* **2007**, 4752−4754. (h) Wang, C.; Chen, Q.; Xu, H.; Wang, Z.; Zhang, X. *Adv. Mater.* **2010**, *22*, 2553−2555.

(4) (a) Ma, N.; Wang, Y. P.; Wang, Z. Q.; Zhang, X. *Langmuir* **2006**, *22*, 3906−3909. (b) Conti, I.; Marchioni, F.; Credi, A.; Orlandi, G.; Rosini, G.; Garavelli, M. *J. Am. Chem. Soc.* **2007**, *129*, 3198−3210. (c) Liu, M.; Yan, X.; Hu, M.; Chen, X.; Zhang, M.; Zheng, B.; Hu, X.; Shao, S.; Huang, F. *Org. Lett.* **2010**, *12*, 2558−2561. (d) Wang, Y.; Bie, F. S.; Jiang, H. *Org. Lett.* **2010**, *12*, 3630−3633. (e) Nguyen, T.-T.-T.; Türp, D.; Wang, D. P.; Nölscher, B.; Laquai, F.; Müllen, K. *J. Am. Chem. Soc.* **2011**, *133*, 11194−11204. (f) Liao, X.; Chen, G.; Jiang, M. *Langmuir* **2011**, *27*, 12650−12656.

(5) (a) Tomatsu, I.; Hashidzume, A.; Harada, A. *J. Am. Chem. Soc.* **2006**, *128*, 2226−2227. (b) Wang, Y. P.; Ma, N.; Wang, Z. Q.; Zhang, X. *Angew. Chem., Int. Ed.* **2007**, *46*, 2823−2826. (c) Liao, X.; Chen, G.; Liu, X.; Chen, W.; Chen, F.; Jiang, M. *Angew. Chem., Int. Ed.* **2010**, *49*, 4409−4413. (d) Jin, H. B.; Zheng, Y. L.; Liu, Y.; Cheng, H.; Zhou, Y. F.; Yan, D. Y. *Angew. Chem., Int. Ed.* **2011**, *50*, 10352−10356. (e) Chen, G.; Jiang, M. *Chem. Soc. Rev.* **2011**, *40*, 2254−2266.

(6) (a) Ogoshi, T.; Kanai, S.; Fujinami, S.; Yamagishi, T. A.; Nakamoto, Y. *J. Am. Chem. Soc.* **2008**, *130*, 5022−5023. (b) Ogoshi, T.; Kitajima, K.; Aoki, T.; Fujinami, S.; Yamagishi, T.; Nakamoto, Y. *J. Org. Chem.* **2010**, *75*, 3268−3273. (c) Zhang, Z.; Xia, B.; Han, C.; Yu, Y.; Huang, F. *Org. Lett.* **2010**, *12*, 3285−3287. (d) Li, C.; Zhao, L.; Li, J.; Ding, X.; Chen, S.; Zhang, Q.; Yu, Y.; Jia, X. *Chem. Commun.* **2010**, *46*, 9016−9018. (e) Zhang, Z.; Luo, Y.; Xia, B.; Han, C.; Yu, Y.; Chen, X.; Huang, F. *Chem. Commun.* **2011**, *47*, 2417−2419. (f) Li, C.; Shu, X.; Li, J.; Chen, S.; Han, K.; Xu, M.; Hu, B.; Yu, Y.; Jia, X. *J. Org. Chem.* **2011**, *76*, 8458−8465. (g) Hu, X.-B.; Chen, L.; Si, W.; Yu, Y. H.; Hou, J.-L. *Chem. Commun.* **2011**, *47*, 4694−4696. (h) Li, C.; Chen, S.; Li, J.; Han, K.; Xu, M.; Hu, B.; Yu, Y.; Jia, X. *Chem. Commun.* **2011**, *47*, 11294−11296. (i) Ma, Y.; Ji, X.; Xiang, F.; Chi, X.; Han, C.; He, J.; Abliz, Z.; Chen, W.; Huang, F. *Chem. Commun.* **2011**, *47*, 12340−12342. (j) Xia, B.; He, J.; Abliz, Z.; Yu, Y.; Huang, F. *Tetrahedron Lett.* **2011**, *52*, 4433−4436. (k) Liu, L.; Cao, D.; Jin, Y.; Tao, H.; Kou, Y.; Meier, H. *Org. Biomol. Chem.* **2011**, *9*, 7007−7010. (l) Zhang, Z.; Luo, Y.; Chen, J.; Dong, S.; Yu, Y.; Ma, Z.; Huang, F. *Angew. Chem., Int. Ed.* **2011**, *50*, 1397−1401. (m) Si, W.; Chen, L.; Hu, X.-B.; Tang, G.; Chen, Z.; Hou, J.-L.; Li, Z.-T. *Angew. Chem., Int. Ed.* **2011**, *50*, 12564−12568. (n) Zhang, Z.; Yu, G.; Han, C.; Liu, J.; Ding, X.; Yu, Y.; Huang, F. *Org. Lett.* **2011**, *13*, 4818−4821. (o) Strutt, N. L.; Forgan, R. S.; Spruell, J. M.; Botros, Y. Y.; Stoddart, J. F. *J. Am. Chem. Soc.* **2011**, *133*, 5668−5671. (p) Cragg, P. J.; Sharma, K. *Chem. Soc. Rev.* **2012**, *41*, 597−607. (q) Li, C.; Han, K.; Li, J.; Zhang, H.; Ma, J.; Shu, X.; Chen, Z.; Weng, L.; Jia, X. *Org. Lett.* **2012**, *14*, 42−45. (r) Yu, G.; Zhang, Z.; Han, C.; Xue, M.; Zhou, Q.; Huang, F. *Chem. Commun.* **2012**, *48*, 2958−2960. (s) Shu, X.; Chen, S.; Li, J.; Chen, Z.; Weng, L.; Jia, X.; Li, C. *Chem. Commun.* **2012**, *48*, 2967−2969. (t) Ogoshi, T.; Shiga, R.; Yamagishi, T.-a. *J. Am. Chem. Soc.* **2012**, *134*, 4577−4580.

(7) (a) Cao, D.; Kou, Y.; Liang, J.; Chen, Z.; Wang, L.; Meier, H. *Angew. Chem., Int. Ed.* **2009**, *48*, 9721−9723. (b) Han, C.; Ma, F.; Zhang, Z.; Xia, B.; Yu, Y.; Huang, F. *Org. Lett.* **2010**, *12*, 4360−4363. (c) Ma, Y.; Zhang, Z.; Ji, X.; Han, C.; He, J.; Abliz, Z.; Chen, W.; Huang, F. *Eur. J. Org. Chem.* **2011**, *27*, 5331−5335. (d) Ma, Y.; Chi, X.; Yan, X.; Liu, J.; Yao, Y.; Chen, W.; Huang, F.; Hou, J.-L. *Org. Lett.* **2012**, *14*, 1532−1535.

(8) Tao, H.; Cao, D.; Liu, L.; Kou, Y.; Wang, L.; Meier, H. *Sci. China, Ser. B: Chem.* **2012**, *55*, 223−228.

(9) Harada, A.; Hashidzume, A.; Yamaguchi, H.; Takashima, Y. *Chem. Rev.* **2009**, *109*, 5974−6023.

(10) (a) Diaz, A.; Quintela, P. A.; Schuette, J. M.; Kaifer, A. E. *J. Phys. Chem.* **1988**, *92*, 3537−3542. (b) Dharmawardana, U. R.; Christian, S. D.; Tucker, E. E.; Taylor, R. W.; Scamehorn, J. F. *Langmuir* **1993**, *9*, 2258−2263. (c) Orihara, Y.; Matsumura, A.; Saito, Y.; Ogawa, N.; Saji, T.; Yamaguchi, A.; Sakai, H.; Abe, M. *Langmuir* **2001**, *17*, 6072−6076.